Seismic performance of RC bridge piers reinforced with varying yield strength steel

Junsheng Su[1,2a], Rajesh Prasad Dhakal[2b], Junjie Wang[*1] and Wenbiao Wang[3c]

[1]*Department of Bridge Engineering, Tongji University, 1239 Siping Rd., Shanghai 200092, PR China*
[2]*Department of Civil and Natural Resources Engineering, University of Canterbury, Private Bag 4800, Christchurch 8140, New Zealand*
[3]*Shanghai Municipal Engineering Design Institute (Group) Co., Ltd., 901 North Zhongshan No.2 Rd., Shanghai, 200093, PR China*

Abstract. This paper experimentally investigates the effect of yield strength of reinforcing bars and stirrups on the seismic performance of reinforced concrete (RC) circular piers. Reversed cyclic loading tests of nine-large scale specimens with longitudinal and transverse reinforcement of different yield strengths (varying between HRB335, HRB500E and HRB600 rebars) were conducted. The test parameters include the yield strength and amount of longitudinal and transverse reinforcement. The results indicate that the adoption of high-strength steel (HSS) reinforcement HRB500E and HRB600 (to replace HRB335) as longitudinal bars without reducing the steel area (i.e., equal volume replacement) is found to increase the moment resistance (as expected) and the total deformation capacity while reducing the residual displacement, ductility and energy dissipation capacity to some extent. Higher strength stirrups enhance the ductility and energy dissipation capacity of RC bridge piers. While the product of steel yield strength and reinforcement ratio ($f_y\rho_s$) is kept constant (i.e., equal strength replacement), the piers with higher yield strength longitudinal bars are found to achieve as good seismic performance as when lower strength bars are used. When higher yield strength transverse reinforcement is to be used to maintain equal strength, reducing bar diameter is found to be a better approach than increasing the tie spacing.

Keywords: High-Strength Steel (HSS) reinforcement; HRB500E; HRB600; seismic performance; ductility; energy dissipation

1. Introduction

The use of high-strength steel (HSS) bars in reinforced concrete (RC) elements offers many advantages, such as reduction of steel congestion and enhancement of bearing capacity, in addition to reduction of costs associated with the transport and placement of reinforcing steel. Thus, RC design codes in many countries have recently exhibited the trend of increasing the yield strength of reinforcement.

In the United States, the permitted yield strength for reinforcing steel has been increased to 550 MPa for longitudinal bars and 700 MPa for confinement reinforcement (ACI 318-14). In the early 1990s, researchers in Japan explored the possibility of using high-strength reinforcement USD685A, USD685B (685 MPa) and USD980 (980 MPa) as axial reinforcement for beams and columns as well as USD785 (785 MPa) and USD1275 (1275 MPa) as lateral reinforcement (Aoyama 2001).

Though these reinforcement types have not yet been accepted by the Japanese Industrial Standard (JIS G 3112 2010), they have gained acceptance through the Ministry of Construction as part of the New RC Construction Standard (Nishiyama 2009, Miyajima 2010). In Europe, the maximum yield strength of steel used in concrete structures is equal to or lower than 600 MPa (CEN 2004, CEN-FIP 2013). The Australian/New Zealand specification (AS/NZS 3101 2006), requires the yield strength of main reinforcement used in design to be equal to or less than 500MPa, while yield strength for confining reinforcement is permitted to be as high as 800 MPa. In China, the reinforcing bars used in design of concrete structures are hot rolled bars (HRB) with distinct yield plateau. The value of yield strength in the current Chinese code for design of concrete structures (GB50010 2010) has been recently increased to 500 MPa (HRB500).

There are two reasons potentially restricting the use of HSS reinforcement in RC structures: (i) crack widths during service conditions; and (ii) ductility capacity for seismic design. Harries *et al*. (2011) and Soltani *et al*. (2013) investigated flexural crack widths of RC members with HSS reinforcement of up to 827 MPa yield strength and concluded that the ACI and AASHTO provisions for crack control were too conservative and could be extended to HSS reinforcement. On the other hand, Shahrooz *et al*. (2013) demonstrated that the strain limits for HSS reinforcement must be changed to achieve the curvature ductility comparable to that implicit with the current use of

*Corresponding author, Professor
  E-mail: jjwang@tongji.edu.cn
[a]Ph.D. Candidate
  E-mail: junshengsu@outlook.com
[b]Professor
  E-mail: rajesh.dhakal@canterbury.ac.nz
[c]MSc.
  E-mail: jiayou0327@126.com

Grade 60 reinforcing steel. This finding led to a number of recommendations that were subsequently incorporated into the AASHTO 2014 specifications (AASHTO 2014).

However, current building codes in many countries contain strict limits regarding the reinforcement strength used in seismic regions due mainly to the lack of research background. For earthquake-resistant design, ACI 318-14 and AASHTO LRFD 2011 specify that Grade 60 (414 MPa) reinforcing steel should be used in members where plastic hinging is expected. Furthermore, for reinforcing steel used in seismic regions, almost all codes impose further restrictions on yield strength, tensile strength, the ratio between measured tensile strength to measured yield strength (f_t/f_y), the ratio between measured yield strength to defined yield strength (f_y/f_{yk}), the percentage total elongation at maximum force (ε) and the percentage elongation after fracture (ε_{rup}), as shown in Table 1. These provisions are intended to ensure ductile behavior of RC structures under earthquake ground motions.

More recently, several researchers have studied the seismic performance of RC members reinforced with HSS reinforcement. In US and Japan, Rautenberg *et al.* (2012, 2013), Cheng *et al.* (2014), Tavallali *et al.* (2014) and Barbosa *et al.* (2015) compared seismic performance of RC members with conventional reinforcement Grade60 (414 MPa) and those with HSS reinforcement Grade80 (550 MPa), Grade100 (690 MPa), Grade120 (827 MPa) or SD685 (685 MPa) with reduced reinforcement dosage. Their experimental results indicated that replacing conventional Grade60 (414) longitudinal steel bars with

proportionally (to the increase in f_y) reduced amounts of HSS reinforcement provided nearly identical moment resistance capacity and comparable deformation capacity.

Considering HSS reinforcement will enhance the yield displacement and thus reduce displacement ductility of RC piers, it appears unfavorable in the conventional ductility measure. It is to be noted here, however, that the HSS reinforcing bars used in Chinese codes are similar to AS/NZS codes, which have better ductility than defined in American and Japanese codes, as shown in Table 1. Recent disastrous earthquakes in China, such as Wenchuan Earthquake in 2008, indicated that rehabilitation of damaged RC structures caused by the excessive post-yield and residual deformation was considerably difficult (Civil and Structural Groups of Tsinghua University *et al.* 2008). For RC structures subjected to earthquake loading, structural resilience is very important for the safety and post-earthquake rehabilitation. Higher yield stress of HSS reinforcement will improve the elastic capacity and reduce residual deformation of RC structures provided sufficient total deformation capacity of the structures is ensured for collapse prevention (Fu *et al.* 2015).

Though many researchers indicated that the use of HSS reinforcement as confining reinforcement could effectively reduce steel consumption in some cases (Razvi and Saatcioglu 1994, Thomson and Wallace 1994, Bing *et al.* 2001, Lin and Lee 2001, Paultre *et al.* 2001, Bayrak and Sheikh 2004, Xiao *et al.* 2008, Shin *et al.* 2016), the benefits of using HSS reinforcement as transverse reinforcement remains a controversial issue as higher strength is likely to lead to a smaller bar diameter or a larger tie spacing, which could reduce the provided confinement stiffness and anti-buckling resistance by transverse reinforcement (Azizinamini *et al.* 1994, Khaloo and Bozorgzadeh 2001, Su *et al.* 2015).

Additionally, due to low carbon and high chromium composition, HSS reinforcement is reported to show better corrosion resistance (Trejo and Pillai 2003, 2004, Clemena and Virmani 2004, Trejo and Monteiro 2005). Thus, it is acceptable to replace conventional steel with HSS reinforcement on a one-to-one basis in some applications on the premise that it has higher moment resistance capacity, deformation capacity and corrosion resistance but is not as costly as stainless steel.

A review of the literature including the extensive PEER column database (Berry and Eberhard 2008) indicates that experimental data on RC members with HSS reinforcement are limited. Especially for the HSS reinforcement used in China, the lack of experimental evidence on the seismic behavior of HSS RC members has been preventing design engineers from utilizing the potential advantages of the HSS reinforcement. The objective of this research is to experimentally explore the potential of using high-strength steels as flexural reinforcement and transverse reinforcement in RC bridge piers without compromising their ductility. The steel used in the piers tested in this investigation included conventional steel HRB335 and high-strength steel HRB500E and HRB600. All the longitudinal steel bars used in the specimens have good ductility as their percentage of total elongation at maximum

Table 1 Mechanical properties of longitudinal reinforcing steel used in seismic regions

Structure standard	Material standard	Grade	d_b (mm)	f_{yk} (MPa)	f_y (MPa)	f_t (MPa)	f_t/f_y	f_y/f_{yk}	ε (%)	ε_{rup} (%)
ACI 318 (2014) AASHTO (2011)	ASTM A615 (2014) ASTM A706 (2014)	Grade 60	10~19		414	≥414 ≤540	≥550	≥1.25		≥14
			22~36							≥12
			43~57							≥10
CEN (2004)		Class B		400 ~600			≥1.08		≥5.0	
		Class C					≥1.15 ≤1.35		≥7.5	
CEB-FIP (2013)		Class C		≤600			≥1.15 ≤1.35	≤1.3	≥7.5	
		Class D					≥1.25 ≤1.45		≥8.0	
AIJ Standard (2010)	JIS G 3112 (2010)	SD490		490	≥490 ≤625	≥620				≥14
AS/NZS 3101 (2006)	AS/NZS 4671 (2001)	500E		500	≥500 ≤600		≥1.15 ≤1.40		≥10	
GB 50011 (2010)	GB 1499.2 (2007)	HRB500E HRBF500E	6~25		500	≥500	≥630	≥1.25	≤1.3	≥9	≥15
			28~36							≥14
			40~50							≥13

Note: d_b is the bar diameter; f_y is the measured yield strength, f_t is the measured tensile strength, f_{yk} is the defined yield strength; ε is the percentage total elongation at maximum force, ε_{rup} is the percentage elongation after fracture

force is more than 9%. Two different steel replacement methods; namely equal volume (one-to-one) and equal strength ($f_{y1}\rho_{s1}=f_{y2}\rho_{s2}$) replacement, were adopted.

The moment resistance, deformation capacity and displacement ductility of RC bridge piers reinforced with high-strength and conventional flexural reinforcement are compared and analyzed to investigate whether the adoption of high-strength steel will affect the ductility of RC bridge piers and the extent of the effect, if there is any. Besides, effects on other aspects of seismic performance such as energy dissipation and residual displacement when high-strength flexural reinforcement is used to replace conventional reinforcement are also discussed. In addition, the sensitivity of seismic performance of RC bridge piers to the yield strength of transverse reinforcement is also scrutinized in this paper. The results of this study can be used to assess the potential use of HRB500E and HRB600 HSS reinforcement in RC bridge piers subjected to seismic loads and can also be used to amend seismic design guidelines for RC bridges.

2. Experimental program

Nine large-scale circular column specimens were tested under cyclic lateral loads while simultaneously subjected to constant axial loads. The slenderness ratio (*L/D*) of the tested specimens was 4.4 and the applied axial load was 760 kN (corresponding to 0.083 and 0.056 axial compression ratio for the C40 and C60 concrete, respectively). The effects of the longitudinal and transverse yield strength on seismic performance of RC bridge piers are investigated while two steel replacement methods; i.e., equal strength and equal volume replacement, are adopted.

2.1 Specimen description

Fig. 1 shows the reinforcement details and the tie configuration in the tested specimens. As can be seen in Table 2, the tested specimens used in this experimental program consisted of nine 600 mm diameter circular piers, the height of which was 2.65 m. The tested series were designed to investigate two main parameters influencing the behavior of piers: (i) the longitudinal bar yield strength; and (ii) the transverse reinforcement yield strength. To identify the steel bars used in different specimens, L, M and H are used to represent the strength of longitudinal and transverse steel, where L, M and H stand for HRB335 (low), HRB500E (medium), and HRB600 (high) steel, respectively. Two different steel replacement methods, equal volume and equal strength replacement, were adopted herein. For equal volume replacement, identical steel configuration and amount were used while only the steel yield strengths were varied. As for equal strength replacement, the products of steel yield strength and reinforcement ratio were kept constant among all specimens, which could be expressed as $f_{y1}\rho_{s1}=f_{y2}\rho_{s2}$. Where equal strength replacement was adopted, the label (S) was used to represent that series.
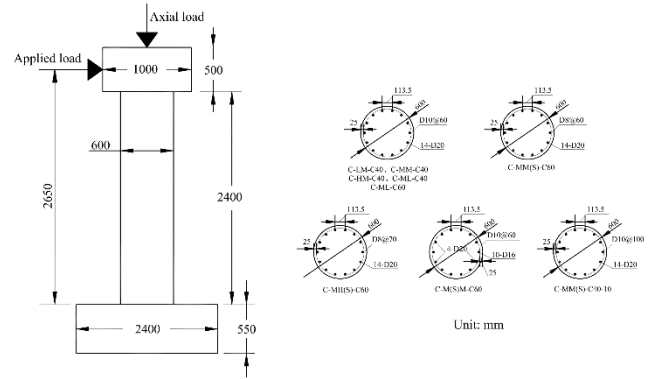

Fig. 1 Geometry and reinforcement details of the test specimens

Table 2 Details of all circular pier test specimens

Specimen	Long. Reinf.				Transv. Reinf.				Class	*P/* kN	*P/P₀*
	d_b/ mm	Class	No.	ρ_l/ %	d_s/ mm	Class	*S/* mm	ρ_s/ %			
C-LM-C40	20	HRB335	14	1.56	10	HRB500E	60	0.80	C40	760	0.083
C-MM-C40	20	HRB500E	14	1.56	10	HRB500E	60	0.80	C40	760	0.083
C-HM-C40	20	HRB600	14	1.56	10	HRB500E	60	0.80	C40	760	0.083
C-M(S)M-C60	20 16	HRB500E	4 10	1.16	10	HRB500E	60	0.80	C60	760	0.056
C-ML-C60	20	HRB500E	14	1.56	10	HRB335	60	0.80	C60	760	0.056
C-MM(S)-C60	20	HRB500E	14	1.56	8	HRB500E	60	0.51	C60	760	0.056
C-MH(S)-C60	20	HRB500E	14	1.56	8	HRB600	70	0.44	C60	760	0.056
C-ML-C40	20	HRB500E	14	1.56	10	HRB335	60	0.80	C40	760	0.083
C-MM(S)-C40-10	20	HRB500E	14	1.56	10	HRB500E	100	0.48	C40	760	0.083

2.2 Material properties

Reinforcing bar detailing of all tested specimens is summarized in Table 3 and stress-strain curves of the steel bars in tension are given in Fig. 2. Each curve in the figure represents an average of three test results. The coupon tests were conducted in accordance of GB/T228.1 (2010). In Table 3, ε_{rup} and ε represent the strain values at rupture and at the maximum force, respectively. Similarly, f_y and f_u are the yield stress and ultimate stress, respectively. We can see from Table 3 and Fig. 2(a) that the high-strength flexural reinforcement HRB500E and HRB600 used herein fulfill the mechanical and ductility requirements shown in Table 1. High-strength longitudinal steel HRB500E and HRB600 both show distinct yield plateau and good ductility even though their ductility are slightly smaller than that of the conventional steel HRB335. Although the transverse reinforcement lack a distinct yield plateau, they possess enough fracture elongation, as shown in Table 3 and Fig. 2(b). The reinforcing cage for each specimen consisted of two parts, one for the pier and the other for the stub. The pier longitudinal bars extended through the stub to 300mm from the base in all specimens.

The concrete strength and elastic modulus of each specimen (Table 4) were obtained by averaging the values obtained in six standard cube tests (150×150×150 mm)

according to GB/T50152 (2012). The concrete cubes were poured and maintained under the same condition as the RC bridge pier specimens.

Table 3 Measured reinforcing material properties

Class	D (mm)	f_y (Mpa)	f_u (MPa)	E_s (MPa)	ε_{rup} (%)	ε (%)
HRB335	10	406	606	1.76×10^5	24.8	8.3
	20	399	543	1.93×10^5	28.3	12.1
HRB500E	8	617	844	1.65×10^5	21.3	7.5
	10	536	729	1.51×10^5	21.2	7.4
	16	499	687	1.93×10^5	24.3	10.9
	20	534	717	1.93×10^5	23.0	10.1
HRB600	8	686	969	1.54×10^5	16.8	6.5
	20	622	777	1.55×10^5	22.4	10.0

Table 4 Measured concrete material properties

Class	$f_c{}'$ (MPa)	E_c (MPa)
C40	32.6	3.32×10^4
C60	48.2	3.62×10^4
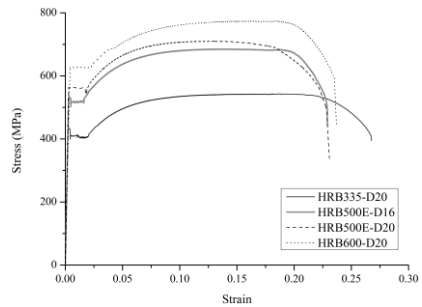
(a) Longitudinal steel
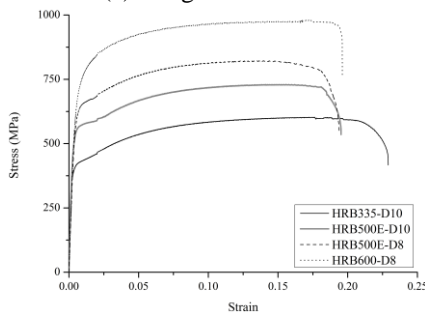

(b) Transverse steel

Fig. 2 Stress-strain behavior of reinforcing steel
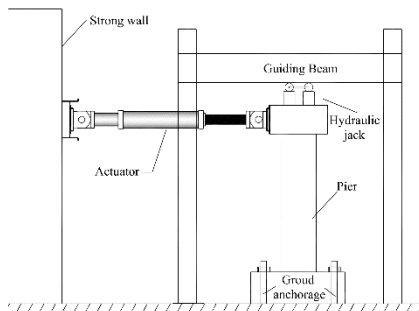

Fig. 3 External instrumentation for RC bridge piers
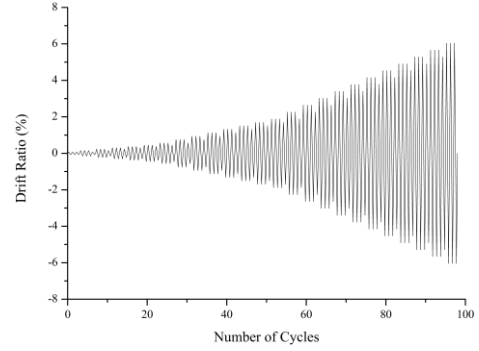
Fig. 4 Loading profile of RC bridge piers

Table 5 Loading profile of RC bridge piers

Main cycle			Minor cycle		
Displacement (mm)	Drift ratio (%)	Number of cycles	Displacement (mm)	Drift ratio (%)	Number of cycles
2	0.08	3			
4	0.15	3	2	0.08	1
6	0.23	3	4	0.15	1
8	0.30	3	6	0.23	1
10	0.38	3	8	0.30	1
12	0.45	3	10	0.38	1
15	0.57	3	12	0.45	1
20	0.75	3	15	0.57	1
25	0.94	3	20	0.75	1
30	1.13	3	25	0.94	1
35	1.32	3	30	1.13	1
40	1.51	3	35	1.32	1
45	1.70	3	40	1.51	1
50	1.89	3	45	1.70	1
60	2.26	3	50	1.89	1
70	2.64	3	60	2.26	1
80	3.02	3	70	2.64	1
90	3.40	3	80	3.02	1
100	3.77	3	90	3.40	1
110	4.15	3	100	3.77	1
120	4.53	3	110	4.15	1
130	4.91	3	120	4.53	1
140	5.28	3	130	4.91	1
150	5.66	3	140	5.28	1
160	6.04	3	150	5.66	1

2.3 Test setup and instrumentation

Test setup initiated with stressing the pier footing to the strong floor with ground anchorage (Fig. 3). The axial compression in the piers was applied to the top of the specimens with a hydraulic jack located between the pier top and a steel reaction beam. The horizontal load was applied by a 1000 kN tension/compression actuator with displacement and force control capabilities, supported

against a reaction wall. The axial load was first applied at the target value and a roller was used to allow for slipping and rotation of the hydraulic jack. The applied axial load was 760 kN, corresponding to 8.3%/5.6% of the nominal axial compression capacity of the specimens with C40/C60 concrete.

A prescribed quasi-static cyclic drift sequence (Fig. 4 and Table 5) was imposed laterally to the top of the specimens. For each maximum drift, three displacement cycles were applied to capture the strength degradation. After three repeated cycles, one small displacement cycle was inserted before increasing the amplitude to the next level. The test was terminated when one of the longitudinal bars ruptured.

3. Experimental results

The test results of the nine specimens were compared to determine the effects of the longitudinal bar and transverse reinforcement yield strengths on seismic performance of RC bridge piers. The moment resistance capacity, drift ratio, displacement ductility, residual displacement and energy dissipation capacity of the tested RC bridge piers are compared in this paper. In all tests, the specimen failed in typical flexural mode which included reinforcing bar buckling followed by longitudinal reinforcing bar fracture.

3.1 General observation

Minor cracks started to occur, first near the base of the specimens, at a top displacement of 6 mm or 8 mm (0.23 or 0.30% drift ratio) (Fig. 5(a)). More cracks then appeared within about 1.5 m from the pier base as the applied drift increased. When the top displacement amplitude reached 15~30 mm (0.75%~0.94% drift ratio), first yielding of a longitudinal rebar occurred, which could be identified by the readings of the strain gages installed on the rebar at the bottom of the pier. When the top displacement further increased, minor spalling of cover concrete at the pier base (Fig. 5(b)) was firstly observed which was soon followed by significant spalling of cover concrete (Fig. 5(c)). The test was continued until buckling and rupture of the longitudinal rebar (Fig. 5(d)) occurred.
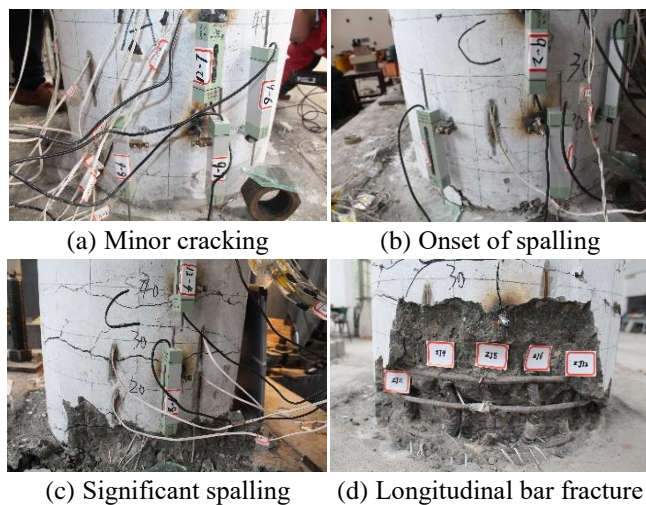
Fig. 6 shows the horizontal force versus drift ratio cyclic plots of all tested RC bridge piers. The hysteresis loops of all tested specimens are ductile and show good energy dissipation except the specimen C-MM(S)-C40-10, whose hysteresis hoop is slightly slim. The lateral load capacity decreased slightly during the repeated cycles corresponding to the same drift amplitude. The moment resistance of RC bridge piers is observed to decrease slowly after the onset of cover concrete spalling and drops suddenly once the bars fractured. The deterioration rate of the moment resistance capacity of the specimens reinforced with high-strength steel is slower than the specimen reinforced with conventional steel. In general, the yield strength of the transverse reinforcement does not seem to have a noticeable effect on the moment resistance and deformation capacity, except that the specimen C-MM(S)-C40-10 has a lesser deformation capacity than other specimens due mainly to the large tie spacing.

In order to further compare the seismic performance of the tested RC bridge piers, other aspects of the hysteresis curves such as drift ratio, displacement ductility, energy dissipation and residual displacement are discussed in the next section.

3.2 Drift capacity, displacement ductility and energy dissipation

Ductility parameters are defined using an idealized load-displacement envelope (Park 1989, Sheikh and Khoury 1993) because the response of a RC bridge pier is far from linear. The nonlinear load-displacement behavior is idealized as a bilinear response, constituting of an elastic branch followed by an inclined inelastic branch (Fig. 7). The yield displacement is calculated according to the

(a) Minor cracking   (b) Onset of spalling

(c) Significant spalling   (d) Longitudinal bar fracture

Fig. 5 Observed damage development progress of RC bridge piers

(a) C-LM-C40   (b) C-MM-C40   (c) C-HM-C40

(d) C-ML-C60   (e) C-MM(S)-C60   (f) C-MH(S)-C60

(g) C-ML-C40   (h) C-MM(S)-C40-10   (i) C-M(S)M-C60
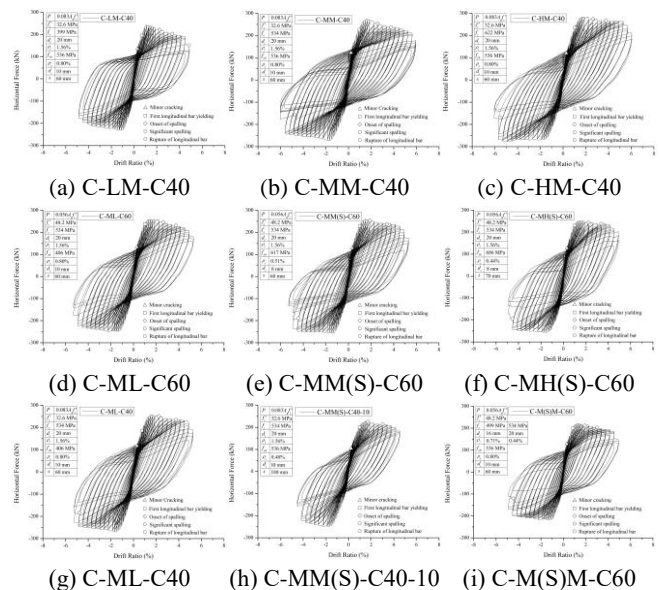
Fig. 6 Shear force versus drift ratio of RC bridge piers
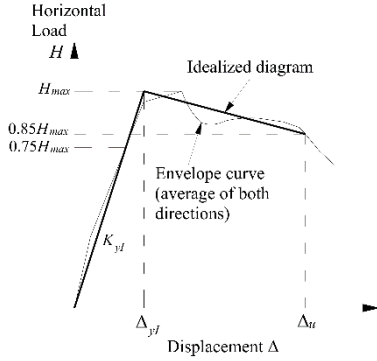
Fig. 7 Idealised bilinear curve definition
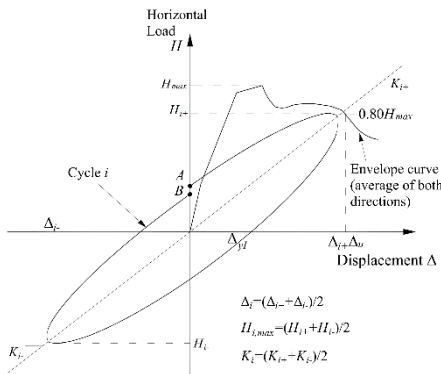
Fig. 8 Energy dissipation

approach suggested by Park (1989), in which the elastic branch crosses the experimental curve at 75% of the maximum horizontal load to define the idealized yield displacement Δ_{yI}. The theoretical failure point is conventionally defined at the post-peak displacement, Δ_u, where the remaining capacity of the pier has dropped to 80% of the peak load (Fig. 7). Displacement ductility μ_Δ is computed as the ratio of the defined failure displacement to the idealized yield displacement, as shown in Eq. (1)

$$\mu_\Delta = \frac{\Delta_u}{\Delta_{yI}} \qquad (1)$$

The maximum drift ratio δ_u consists of elastic and inelastic deformation and is a more direct parameter to define deformation capacity, which is defined as in Eq. (2)

$$\delta_u = \frac{\Delta_u}{L} \qquad (2)$$

where the pier height $L=2.65$ m. It is generally assumed that a drift ratio of about 4% represents a very good level of ductility (Mirza *et al.* 1996).

Energy dissipation capacity is associated with the force-displacement response and is an important parameter in the seismic design of RC structures. The energy dissipation for a response cycle i is defined by the hatched area as shown in Fig. 8 or expressed mathematically as

$$E_i = \iint_A^B H d\Delta \qquad (3)$$

The total energy E_{hyst} dissipated during the test is the

Table 6 Summary of moment resistance, deformation, ductility, energy dissipation index

Specimen	Δ_{yI} (mm)	H_{max} (kN)	Δ_u (mm)	δ_u (%)	μ_Δ	E_{hyst} (kJ)	E_N	I_W	D_{EW}
C-LM-C40	20.6	237	121.2	4.57	5.88	967	157	119	566
C-MM-C40	28.7	274	147.3	5.56	5.14	1354	141	119	467
C-HM-C40	32.4	282	155.9	5.88	4.81	1434	130	118	425
C-M(S)M-C60	20.2	220	126.3	4.77	6.26	936	169	133	674
C-ML-C60	24.1	255	133.3	5.03	5.52	1021	138	121	492
C-MM(S)-C60	26.1	258	132.8	5.01	5.09	1068	127	112	423
C-MH(S)-C60	23.5	255	130.4	4.92	5.54	1055	141	120	506
C-ML-C40	27.3	264	137.5	5.19	5.03	1170	130	113	423
C-MM(S)-C40-10	28.3	239	113.9	4.30	4.03	607	73	80	197

sum of E_i over n cycles to failure, as shown in Eq. (4)

$$E_{hyst} = \sum_{i=1}^{n} E_i \qquad (4)$$

For comparison purposes, the normalized total dissipated energy defined by Paulay *et al.* (1982) is adopted herein. In this approach, H_{max} is the maximum lateral load and Δ_{yI} is the idealized yield displacement, as shown in Fig. 7

$$E_N = \frac{1}{H_{max}\Delta_{yI}} \sum_{i=1}^{n} E_i \qquad (5)$$

Energy dissipation and inelastic deformation capabilities may also be assessed by work index. The work index I_W proposed by Gosain *et al.* (1977) is defined as

$$I_W = \sum_{i=1}^{n} \frac{H_i \Delta_i}{H_{max}\Delta_{yI}} \qquad (6)$$

The normalized energy index D_{EW} proposed by Ehsani and Wright (1990) combines the cyclic dissipated energy and the elastic energy as

$$D_{EW} = \frac{1}{H_{max}\Delta_{yI}} \sum_{i=1}^{n} E_i \left(\frac{K_i}{K_y}\right)\left(\frac{\Delta_i}{\Delta_{yI}}\right)^2 \qquad (7)$$

where K_i and Δ_i are defined in Fig. 8.

4. Analysis of results

4.1 Effect of steel equal volume replacement

4.1.1 Longitudinal bar equal volume replacement

In this series, the geometry and the longitudinal as well as the transverse reinforcement configurations were kept same while longitudinal bar yield strength was increased from 399 MPa to 534 MPa and 622 MPa for specimens C-

LM-C40, C-MM-C40 and C-HM-C40, respectively. It can be observed from Table 6 and Fig. 9 that the yield displacement, moment resistance, drift capacity and total energy dissipation of RC bridge piers increase with an increase in longitudinal steel yield strength. With the yield strength of steel f_y increased by 34% and 56%, the idealized yield displacement Δ_{yI} and the total energy dissipation E_{hyst} increase by 39% and 57%, and 40% and 48%, respectively. The increase in lateral bearing capacity H_{max} and ultimate drift ratio δ_u are 16% and 19%, 22% and 29%, respectively for the two cases, which are slightly smaller than the increase in steel yield strength f_y. Consequently, the displacement ductility μ_Δ decreases by 13% and 18% for RC piers reinforced with high-strength steel HRB500E and HRB600 compared with the conventional steel HRB335.

The greater yield stress f_y of HSS improves the elastic deformation of the RC bridge piers, and this causes less energy to be dissipated at the same total deformation, as shown in Fig. 9(b). The normalized energy dissipation indexes E_N and D_{EW} decrease with the increase of steel yield strength because of the increase in the moment resistance capacity H_{max} and also the idealized yield displacement Δ_{yI} at the same time. However, the energy dissipation index I_W is almost unchanged for specimens C-LM-C40, C-MM-C40 and C-HM-C40, as listed in Table 6. It can be observed that the value of $E_{hyst}/H_i\Delta_i$ decreases with an increase in steel yield strength, which means that the hysteresis loops become slimmer and represent relatively poorer energy dissipation capacity for RC bridge piers with higher strength longitudinal bars. On the other hand, the adaption of HSS reinforcement is found to enhance the elastic capacity and reduce the residual deformation of the RC bridge piers at a given total deformation, as shown in Fig. 9(d). The reduction of residual deformation and enhancement of elastic capacity lead to reduction in damage, which is good for rehabilitation of damaged RC bridge piers following an earthquake.
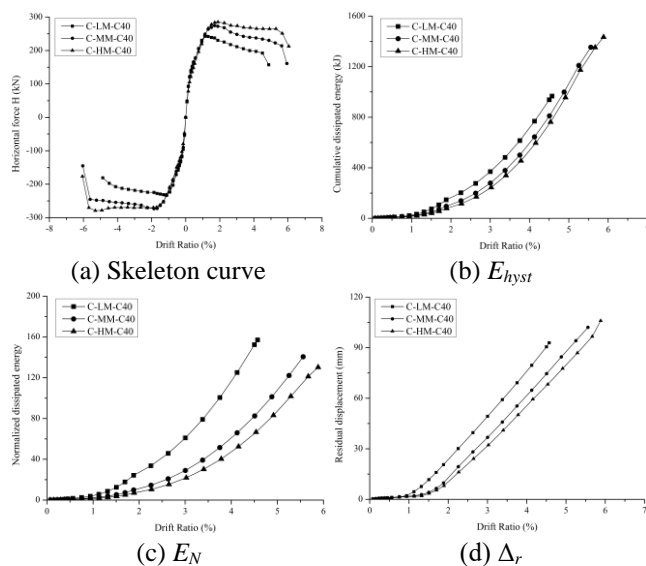
4.1.2 Transverse reinforcement equal volume replacement

For RC bridge pier specimens C-ML-C40 and C-MM-C40, the cross section, longitudinal bar and transverse reinforcement configurations and longitudinal bar yield strength were same while the transverse reinforcement yield strength was increased from 406 MPa to 536 MPa. The load-displacement envelope curves are almost overlapping until the failure point, as shown in Fig. 10(a). The ultimate drift ratio δ_u and energy dissipation E_{hyst} increase by 7% and 16% respectively when the stirrups' yield strength increases by 32% from 406 MPa to 536 MPa. It is because that stronger stirrups can improve the effective confinement to core concrete and also provide better resistance against bar buckling; thereby enhancing the pier's overall deformability. The energy dissipation E_{hyst} and residual displacement Δ_r present similar trend with the skeleton curves being almost identical until failure for the specimens with different yield strength transverse reinforcement, as shown in Fig. 10(b) and Fig. 10(d).

4. 2 Effect of steel equal strength replacement

4.2.1 Longitudinal bar equal strength replacement

The effect of steel yield strength (while keeping the total strength constant) can be investigated from Fig. 11 and Table 6. For specimen C-LM-C40, the longitudinal steel yield strength was 399 MPa and the concrete strength was 32.6 MPa, while 499/534 MPa yield strength longitudinal steel bar and 48.2 MPa strength concrete were adopted in specimen C-M(S)M-C60. The cross section as well as the amount and configuration of the transverse reinforcement were identical for these two specimens. Note that although in the two specimens, the steel replacement basis was to have the same value of $f_y\rho_s$ and lateral bearing capacity H_{max}, the calculated value of $f_y\rho_s$ and the measured maximum lateral load H_{max} of the specimen C-M(S)M-C60
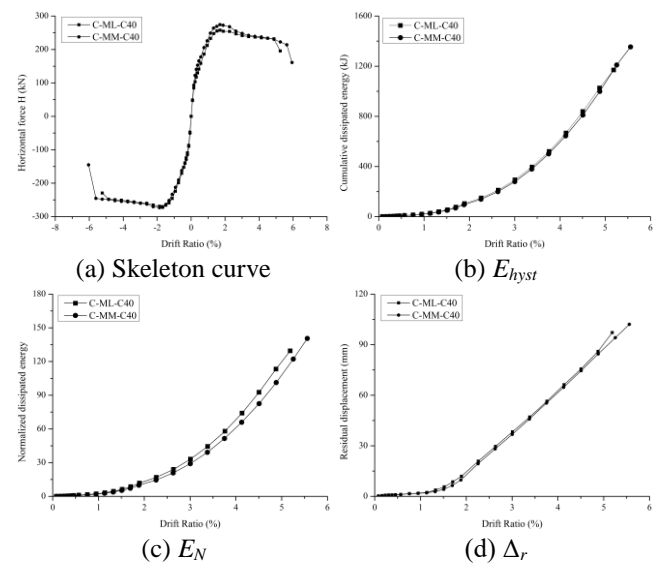

(a) Skeleton curve   (b) E_{hyst}

(c) E_N (d) Δ_r

Fig. 9 Effect of longitudinal bar equal volume replacement

(a) Skeleton curve   (b) E_{hyst}

(c) E_N (d) Δ_r

Fig. 10 Effect of transverse reinforcement equal volume replacement

(a) Skeleton curve

(b) E_{hyst}

(c) E_N

(d) Δ_r

Fig. 11 Effect of longitudinal bar equal strength replacement

(a) Skeleton curve

(b) E_{hyst}

(c) E_N

(d) Δ_r

Fig. 12 Effect of transverse reinforcement equal strength replacement (different diameter)
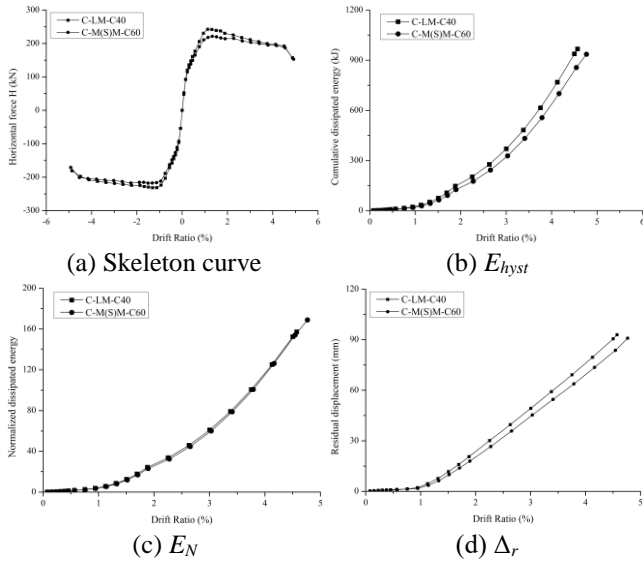
are 10% and 7% smaller than the corresponding values for specimen C-LM-C40.

Due to a slight decrease of the idealized yield displacement Δ_{yI}, the displacement ductility μ_Δ is slightly higher for piers reinforced with higher yield strength steel, as shown in Table 6. The total energy dissipation E_{hyst} of RC piers reinforced with high-strength steel is smaller, because of the smaller lateral bearing capacity H_{max}. Owing to the counterbalancing effect of the lower lateral bearing capacity H_{max} and smaller total energy dissipation E_{hyst}, the normalized dissipation E_N of specimen C-M(S)M-C60 is almost identical to specimen C-LM-C40 at the same drift ratio δ, as illustrated in Fig. 11(c). In the meantime, the pier with HSS reinforcement (HRB500E) shows lower residual deformation Δ_r when compared with the pier constructed with conventional steel (HRB335), as shown in Fig. 11(d).

Overall, seismic performance of piers constructed with HSS reinforcement (HRB500E) is as good as that of piers constructed with conventional steel (HRB335) when equal strength replacement is adopted.

4.2.2 Transverse reinforcement equal strength replacement

Two different steel replacement methods were applied for transverse reinforcement equal strength replacement. As per these two approaches, the specimen with higher strength stirrups could be provided with: either the same tie spacing and smaller bar diameter or the same bar diameter but wider tie spacing.

For specimens C-ML-C60, C-MM(S)-C60 and C-MH(S)-C60, the yield strength of the transverse reinforcement increased from 406 MPa to 617 MPa and 686 MPa while the corresponding bar (stirrup) diameters were 10 mm, 8 mm and 8 mm respectively. The former two specimens had 6 cm tie spacing while the third specimen had 7 cm tie spacing.

Table 6 and Fig. 12 show that the skeleton curves, energy dissipation index (E_{hyst}) curves and residual
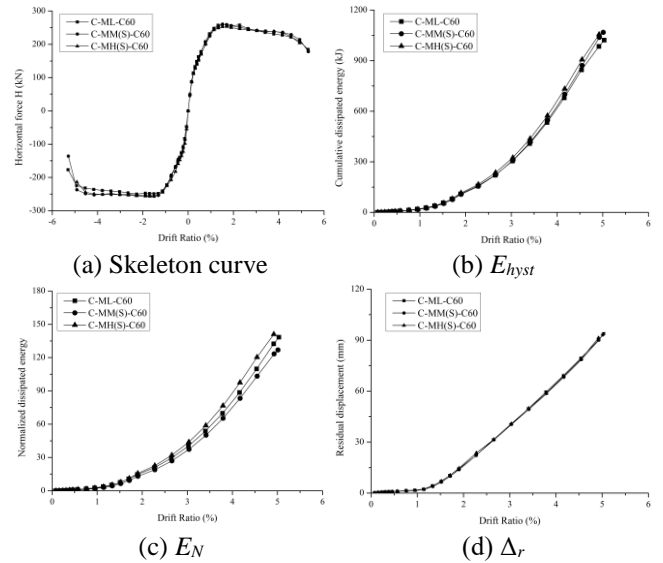
deformations (Δ_r) curves almost completely overlap for these three specimens. Normalized energy dissipation E_N shows only a minor change with variation of transverse steel yield strength. These observations indicate that changing the yield strength and diameter of transverse reinforcement while keeping the product of the yield strength and the stirrup area constant has no significant effect on seismic performance of RC bridge piers as long as the stirrup arrangement and spacing are not altered.

For specimen C-ML-C40 and C-MM(S)-C40-10, the tie spacing S increased from 6 cm to 10 cm when the transverse steel yield strength f_y increased from 406 MPa to 536 MPa. Note that although the steel replacement was designed for equal strength replacement ($f_{y1}\rho_{s1}=f_{y2}\rho_{s2}$), the value of $f_y\rho_s$ calculated by using the measured yield strength is 20% smaller for RC piers reinforced with high-strength steel than that with conventional steel.

According to Table 6 and Fig. 13, the drift capacity and the total energy dissipation capacity drop significantly with increase of tie spacing; the ultimate drift ratio δ_u and displacement ductility μ_Δ decreased by 17% and 20%, respectively. Owing to the reduction of ductility, the total energy dissipation E_{hyst} and normalized indexes E_N drop by 48% and 44%, respectively. However, the normalized energy dissipation E_N and residual displacements Δ_r of the two piers are almost equal for these two specimens at the same total deformation.

According to section 4.1.2, the influence of steel strength on seismic performance of RC piers is limited when tie spacing is kept constant for equal volume replacement (stirrup). The transverse equal strength replacement with the same tie spacing also shows almost no influence on seismic performance for RC bridge piers. Thus, even though the product of $f_y\rho_s$ for RC piers reinforced with higher strength steel is smaller to some extent for transverse equal strength replacement with different tie spacing, the significant decrease in displacement ductility μ_Δ and energy dissipation capacity

(a) Skeleton curve

(b) E_{hyst}

(c) E_N

(d) Δ_r
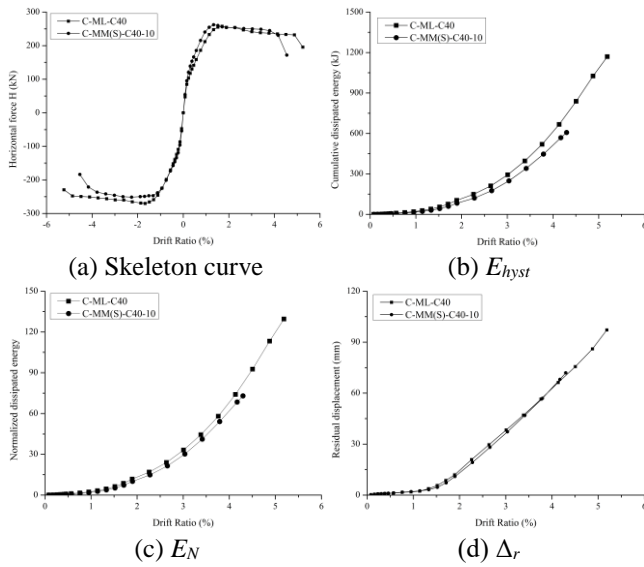
Fig. 13 Effect of transverse reinforcement equal strength replacement (different spacing)

E_{hyst} are mainly caused by the increase of tie spacing when higher strength steel is used.

Comparing the outcomes of the two approaches of equal strength replacement (stirrup), it is clear that reducing steel diameter results in a better performance than increasing tie spacing. It is because reinforcement buckling and subsequent fracture of bars is the main failure mode for RC bridge piers with good confinement. Increasing stirrups spacing has a more adverse influence on bar buckling than reducing the stirrup diameter (Su *et al.* 2015). Hence, as bar buckling is a critical factor governing seismic performance of RC bridge piers, reducing bar diameter (rather than increasing the tie spacing) is a better choice in stirrups replacement.

These observations indicate that the adaption of high-strength bars as flexural reinforcement will reduce residual displacement while the yield strength of transverse reinforcement has no effect on residual displacements of RC piers at the same total deformation.

5. Conclusions

Seismic performance of RC bridge piers with high-strength reinforcement are experimentally assessed and compared with the seismic performance of similar piers with normal strength reinforcement. Comparison is made in terms of key performance indexes such as ultimate drift ratio, displacement ductility, energy dissipation and residual deformation of the RC bridge piers. The variables in the nine different specimens tested in this research included longitudinal and transverse reinforcement yield strength. In varying the yield strength of the reinforcement, the amount of longitudinal and transverse steel was calculated to ensure equal strength (constant $f_y\rho_s$) and equal volume (constant ρ_s) in the different specimens. Based on the results of the extensive experimental investigation reported in this paper, the following conclusions can be made.

• When HSS longitudinal bars (HRB500E, HRB600) are used to replace conventional steel (HRB335) with equal volume (one-to-one) replacement, the moment resistance expectedly increases. While the total deformation capacity of the piers is found to increase with high strength reinforcement, the residual displacement decreases. All RC bridge piers show typical ductile failure even though the application of HSS steel reduces the ductility and energy dissipation capacity of RC bridge piers to some extent.

• The deformation capacity and energy dissipation capacity are found to increase when HSS reinforcement (HRB500E) is used to replace conventional steel (HRB335) as transverse reinforcement with equal volume. It is because HSS reinforcement could supply better confinement to core concrete and restraint against buckling of longitudinal bars.

• Considering better corrosion resistance of HSS reinforcement, the one-to-one (i.e., equal volume) replacement could be acceptable in coastal regions to replace conventional steel even though slightly higher costs while it could enhance seismic performance of RC bridge piers.

• The piers constructed with HSS reinforcement (HRB500E) longitudinal bars have been found to achieve as good moment resistance, deformation capacity, ductility and energy dissipation capacity as, and smaller residual displacement than, the piers constructed with conventional steel (HRB335) designed for the same strength.

• The deformation, ductility, energy dissipation and residual displacement are almost identical when the tie spacing is kept same and smaller bar diameter is used as per equal strength replacement of stirrups of different yield strength. On the other hand, if the same bar diameter and bigger tie spacing is employed, the drift ratio, ductility and energy dissipation capacity reduce substantially.

• Although both are consistent with the equal strength approach, smaller bar diameter and unchanged tie spacing is a better method to accommodate stirrups made of high yield strength bars in RC bridge piers than using the same bar diameter and bigger tie spacing. It is because that bar buckling has a significant influence on seismic performance of RC bridge piers and tie spacing has bigger influence on bar buckling than the stirrup diameter.

• The use of high-strength longitudinal bar could reduce the residual displacement of RC bridge piers compared to that reinforced with conventional steel at same total deformation. The yield strength and configuration of transverse reinforcement, however, show minor effect on moment resistance, energy dissipation and residual displacement of RC piers at the same drift ratio. Hence, based on this investigation, it can be concluded that the use of high strength bars in RC bridge piers does not compromise any aspects of their seismic performance and brings in new benefits such as potential reduction in member sizes, improved corrosion resistance, less amount of steel to be transported/caged, ease in concrete

pouring etc.

References

AASHTO (2011), *AASHTO guide specifications for LRFD seismic bridge design*, American Association of State Highway and Transportation Officials, Washington DC.

AASHTO (2014), *AASHTO LRFD bridge design specifications*, (6th Edition), American Association of State Highway and Transportation Officials, Washington DC.

ACI 318 (2014), 318-14: *Building code requirements for structural concrete*, American Concrete Institute, Farmington Hills, MI.

AIJ Standard (2010), *Standard for structural calculation of reinforced concrete structures-based on allowable stress concept*, Architectural Institute of Japan, Tokyo, Japan.

Aoyama, H. (2001), *Design of Modern Highrise Reinforced Concrete Structures*, Imperial College Press, London, UK.

AS/NZS 4671 (2001), *Steel reinforcing materials*, Australian/New Zealand Standard, Sydney/Wellington, Australia/New Zealand.

ASTM A615 (2014), *Standard specification for deformed and plain carbon-steel bars for concrete reinforcement*, ASTM International, West Conshohocken, PA.

ASTM A706 (2014), *Standard specification for deformed and plain low-alloy steel bars for concrete reinforcement*, ASTM International, West Conshohocken, PA.

Azizinamini, A., Kuska, S.S.B., Brungardt, P. and Hatfield, E. (1994), "Seismic behavior of square high-strength concrete columns", *ACI Struct. J.*, **91**(3), 336-345.

Barbosa, A.R., Link, T. and Trejo, D. (2015), "Seismic performance of high-strength steel RC bridge columns", *J. Bridge Eng.*, **21**(2), 04015044.

Bayrak, O. and Sheikh, S.A. (2004), "Seismic performance of high strength concrete columns confined with high strength steel", *13th World Conference on Earthquake Engineering*, Vancouver, BC, August.

Berry, M.P. and Eberhard, M.O. (2008), Performance modeling strategies for modern reinforced concrete bridge columns, *Rep. No. PEER 2007/07*, Pacific Earthquake Engineering Research Center, Univ. of California, Berkeley, CA.

Bing, L., Park, R. and Tanaka, H. (2001), "Stress-strain behavior of high-strength concrete confined by ultra-high-and normal-strength transverse reinforcements", *ACI Struct. J.*, **98**(3), 395-406.

CEN (2004), *Design of concrete structures: part 1-1: general rules and rules for buildings*, Comité Européen de Normalisation/European Committee for Standardization, Brussels, Belgium.

CEN-FIP (2013), *fib Model code for concrete structures 2010*, Fédération Internationale du Béton/International Federation for Structural Concrete (*fib*), Lausanne, Switzerland.

Cheng, M.Y. and Giduquio, M.B. (2014), "Cyclic behavior of reinforced concrete flexural members using high-strength flexural reinforcement", *ACI Struct. J.*, **111**(4), 893-902.

Civil and structural groups of Tsinghua University, Xi'an Jiaotong University and Beijing Jiaotong University (2008), "Analysis on seismic damage of buildings in the Wenchuan Earthquake", *J. Build. Struct.*, **29**(4), 1-9.

Clemena, G.G. and Virmani, Y.P. (2004), "Comparing the chloride resistances of reinforcing bars", *Concrete Int.*, **26**(11), 39-49.

Ehsani, M. and Wight, J. (1990), "Confinement steel requirements for connections in ductile frames", *J. Struct. Eng.*, **116**(3), 751-767.

Fu, J., Wu, Y. and Yang, Y.b. (2015), "Effect of reinforcement strength on seismic behavior of concrete moment frames", *Earthq. Struct.*, **9**(4), 699-718.

GB 1499.2 (2007), *Steel for the reinforcement of concrete-part 2: hot rolled ribbed bars*. Standardization Administration of the People' Republic of China & General Administration of Quality Supervision, Inspection and Quarantine of the People's Republic of China, Beijing, China.

GB 50010 (2010), *Code for design of concrete structures*, Ministry of Housing and Urban-rural Development, Beijing, China.

GB 50011 (2010), *Code for seismic design of buildings*, Ministry of Housing and Urban-rural Development, Beijing, China.

GB/T228.1 (2010), *Metallic materials-tensile testing-part 1: method of test at room temperature*, Standardization Administration of the People' Republic of China & General Administration of Quality Supervision, Inspection and Quarantine of the People's Republic of China, Beijing, China.

GB/T50152 (2012), *Standard for test method of concrete structures*, China Architecture & Building Press, Beijing, China.

Gosain, N.K., Brown, R.H. and Jersa, J. (1977), "Shear requirements for load reversals on RC members", *J. Struct. Div.*, **103**(7),1461-1476.

Harries, K.A., Shahrooz, B.M. and Soltani, A. (2011), "Flexural crack widths in concrete girders with high-strength reinforcement", *J. Bridge Eng.*, **17**(5), 804-812.

JIS G 3112 (2010), *Steel bars for concrete reinforcement*, Japanese Industrial Standards Committee, Tokyo, Japan.

Joint ACI-ASCE Committee (1997), "High-Strength Concrete Columns: State of the Art", *Rep. No. ACI 441R-96, ACI Struct. J.*, **94**(6), 323-335.

Khaloo, A.R. and Bozorgzadeh, A. (2001), "Influence of confining hoop flexural stiffness on behavior of high-strength lightweight concrete columns", *ACI Struct. J.*, **98**(5), 657-664.

Lin, C.H. and Lee, F.S. (2001), "Ductility of high-performance concrete beams with high-strength lateral reinforcement", *ACI Struct. J.*, **98**(4), 600-608.

Miyajima, M. (2010), "The Japanese experience in design and application of seismic grade rebar", *Proceedings of Int. Seminar on Production and Application of High Strength Seismic Grade Rebar Containing Vanadium*, Beijing, June.

Nishiyama, M. (2009), "Mechanical properties of concrete and reinforcement state-of-the-art report on HSC and HSS in Japan", *J. Adv. Concrete Tech.*, **7**(2), 157-182.

NZS 3101 (2006), *Concrete structures standard-part 1: the design of concrete structures*, New Zealand Standard, Wellington, New Zealand.

Park, R. (1989), "Evaluation of ductility of structures and structural assemblages from laboratory testing", *B. New Zeal. Natl. Soc. Earthq. Eng.*, **22**(3), 155-166.

Paulay, T., Priestley, M. and Synge, A. (1982), "Ductility in earthquake resisting squat shearwalls", *ACI Struct. J.*, **79**(4), 257-269.

Paultre, P., Legeron, F. and Mongeau, D. (2001), "Influence of concrete strength and transverse reinforcement yield strength on behavior of high-strength concrete columns", *ACI Struct. J.*, **98**(4), 490-501.

Rautenberg, J.M., Pujol, S., Tavallali, H. and Lepage, A. (2012), "Reconsidering the use of high-strength reinforcement in concrete columns", *Eng. Struct.*, **37**, 135-142.

Rautenberg, J.M., Pujol, S., Tavallali, H. and Lepage, A. (2013), "Drift capacity of concrete columns reinforced with high-strength steel", *ACI Struct. J.*, **110**(2), 307-317.

Razvi, S.R. and Saatcioglu, M. (1994), "Strength and deformability of confined high-strength concrete columns", *ACI Struct. J.*, **91**(6), 678-687.

Shahrooz, B.M., Reis, J.M., Wells, E.L., Miller, R.A., Harries, K.A. and Russell, H.G. (2013), "Flexural members with high-strength reinforcement: behavior and code implications", *J. Bridge Eng.*, **19**(5), 04014003.

Sheikh, S.A. and Khoury, S.S. (1993), "Confined concrete columns with stubs", *ACI Struct. J.*, **90**(4), 414-431.

Shin, H.O., Yoon, Y.S., Cook, W.D. and Mitchell, D. (2016), "Axial load response of ultra-high-strength concrete columns and high-strength reinforcement", *ACI Struct. J.*, **113**(2), 325-336.

Soltani, A., Harries, K.A. and Shahrooz, B.M. (2013), "Crack opening behavior of concrete reinforced with high strength reinforcing steel", *Int. J. Concrete Struct. Mater.*, **7**(4), 253-264.

Su, J., Wang, J., Bai, Z., Wang, W. and Zhao, D. (2015), "Influence of reinforcement buckling on the seismic performance of reinforced concrete columns", *Eng. Struct.*, **103**, 174-188.

Tavallali, H., Lepage, A., Rautenberg, J.M. and Pujol, S. (2014), "Concrete beams reinforced with high-strength steel subjected to displacement reversals", *ACI Struct. J.*, **111**(5), 1037-1047.

Thomson, J.H. and Wallace, J.W. (1994), "Lateral load behavior of reinforced concrete columns constructed using high-strength materials", *ACI Struct. J.*, **91**(5), 605-615.

Trejo, D. and Monteiro, P.J. (2005), "Corrosion performance of conventional (ASTM A615) and low-alloy (ASTM A706) reinforcing bars embedded in concrete and exposed to chloride environments", *Cement Concrete Res.*, **35**(3), 562-571.

Trejo, D. and Pillai, R.G. (2003), "Accelerated chloride threshold testing: Part I-ASTM A 615 and A 706 reinforcement", *ACI Mater. J.*, **100**(6), 519-527.

Trejo, D. and Pillai, R.G. (2004), "Accelerated chloride threshold testing: Part II-corrosion-resistant reinforcement", *ACI Mater. J.*, **101**(1), 57-64.

Xiao, X., Guan, F. and Yan, S. (2008), "Use of ultra-high-strength bars for seismic performance of rectangular high-strength concrete frame columns", *Mag. Concrete Res.*, **60**(4), 253-259.

AG